



Cite this: *Biomater. Sci.*, 2023, **11**, 2661

## Biomedically-relevant metal organic framework-hydrogel composites

Jason Y. C. Lim, \*†<sup>a,b</sup> Leonard Goh, <sup>†</sup><sup>a</sup> Ken-ichi Otake, <sup>a,c</sup> Shermin S. Goh, <sup>a</sup> Xian Jun Loh <sup>a,b</sup> and Susumu Kitagawa \*<sup>a,c</sup>

Metal organic frameworks (MOFs) are incredibly versatile three-dimensional porous materials with a wide range of applications that arise from their well-defined coordination structures, high surface areas and porosities, as well as ease of structural tunability due to diverse compositions achievable. In recent years, following advances in synthetic strategies, development of water-stable MOFs and surface functionalisation techniques, these porous materials have found increasing biomedical applications. In particular, the combination of MOFs with polymeric hydrogels creates a class of new composite materials that marries the high water content, tissue mimicry and biocompatibility of hydrogels with the inherent structural tunability of MOFs in various biomedical contexts. Additionally, the MOF–hydrogel composites can transcend each individual component such as by providing added stimuli-responsiveness, enhancing mechanical properties and improving the release profile of loaded drugs. In this review, we discuss the recent key advances in the design and applications of MOF–hydrogel composite materials. Following a summary of their synthetic methodologies and characterisation, we discuss the state-of-the-art in MOF–hydrogels for biomedical use – cases including drug delivery, sensing, wound treatment and biocatalysis. Through these examples, we aim to demonstrate the immense potential of MOF–hydrogel composites for biomedical applications, whilst inspiring further innovations in this exciting field.

Received 19th November 2022,  
Accepted 31st January 2023

DOI: 10.1039/d2bm01906j

[rsc.li/biomaterials-science](http://rsc.li/biomaterials-science)

## 1. Introduction

Metal–organic frameworks (MOFs),<sup>1</sup> also known as porous coordination polymers (PCPs),<sup>2</sup> are porous materials composed of metal nodes connected by organic linkers. Despite being known since 1965, interest in these crystalline nanoporous materials only exploded after their synthesis by reticular chemistry was established.<sup>3,4</sup> Owing to their advantageous combinations of high porosity, large surface areas, ease of bottom-up structural tunability at the atomic level and wide range of pore sizes and topologies,<sup>5</sup> MOFs are well-established in applications such as gas uptake and storage,<sup>6–8</sup> carbon capture and conversion,<sup>9</sup> catalysis<sup>10</sup> and molecular sensing.<sup>11</sup> The development of these porous materials have witnessed evolution over several generations. While first generation

coordination networks lack permanent porosity, second generation MOFs have stable frameworks where porosities are maintained regardless of guest presence within the pores. Third generation MOFs represent the next stage in MOF development, achieving properties such as structural flexibility and dynamism, and allowing responses to external physical and chemical stimuli. Increasingly, there is growing interest in interdisciplinary research into how MOFs can be utilised, in what is termed as the ‘fourth generation of MOFs’<sup>12,13</sup> or ‘new age of MOFs’.<sup>14</sup> Here, hybridisation of MOFs with other materials, such as polymers, to form composites is an important theme, which combines and transcends the properties of individual components. These attributes guide the increasingly-important applications of MOFs in the biomedical field,<sup>15</sup> with seminal early studies reported for drug delivery<sup>16–19</sup> and imaging.<sup>17,20,21</sup> Within the last decade, more sophisticated biomedical applications of MOFs in biosensing<sup>22</sup> and biocatalysis<sup>23</sup> have been explored. In addition, the confluence of nanotechnology and MOFs gives rise to nanoscale MOFs (nMOFs) which are commonly utilised in biomedical applications due to their much greater porosity and larger capacity.<sup>24</sup> The intersection with polymer chemistry leads to MOF–polymer hybrids that often have synergistic benefits from both materials.<sup>25</sup> Of particular interest in biomedical applications is the incorporation of MOFs into hydrogels

<sup>a</sup>Laboratory for Green Porous Materials, Institute of Materials Research and Engineering (IMRE), Agency for Science, Technology and Research (A\*STAR), 2 Fusionopolis Way, Innovis #08-03, Singapore 136834, Republic of Singapore.

E-mail: [kitagawa@icems.kyoto-u.ac.jp](mailto:kitagawa@icems.kyoto-u.ac.jp), [jason\\_lim@imre.a-star.edu.sg](mailto:jason_lim@imre.a-star.edu.sg)

<sup>b</sup>Department of Materials Science and Engineering, National University of Singapore (NUS), 9 Engineering Drive, Singapore 117576, Republic of Singapore

<sup>c</sup>Institute for Integrated Cell-Material Sciences, Kyoto University Institute for Advanced Study, Kyoto University, Yoshida Ushinomiya-cho, Sakyo-ku, Kyoto 606-8501, Japan

†These authors contributed equally to the manuscript.



which has gained considerable interest as a hybrid material in the past decade that has been used for  $\text{CO}_2$  capture, water treatment, biomass degradation and adsorption.<sup>26</sup>

Hydrogels are soft materials comprising of three-dimensional crosslinked networks of small molecule gelators or polymers containing large amounts of water. The high water content and flexible nature of hydrogels mimic living tissues well<sup>27</sup> which makes them ideal candidates for biomedical applications. Hydrogels are highly suited for drug delivery applications, biological matrices for wound healing and tissue recovery.<sup>28–30</sup> Inclusion of MOFs into hydrogels can expand the range of applications of hydrogels. In certain cases, the hydrogels serve as reservoirs for the MOFs to regulate release of therapeutic payloads such that they can achieve beneficial medical outcomes while not becoming cytotoxic to the host cells.<sup>31</sup> Conversely, MOFs can improve the mechanical properties of the hydrogels to make them more suitable for applications such as drug delivery.<sup>32</sup> The benefits of MOFs-containing hydrogels go both ways and they are highly complementary.

MOFs are generally perceived to possess a number of limitations which thwart their applications in aqueous media, including hydrogel formulations. Firstly, considering the hydrolytic instability of many MOFs, it would seem paradoxical to incorporate them into hydrogels as it might potentially lead to decomposition of the MOFs. To utilise MOFs for biomedical applications, the MOFs must be stable in aqueous medium to be effective. This might limit the type of MOFs that can be included in hydrogels. Several efforts have been made to address this problem, as evident by the increasing number of reports of water-stable MOFs.<sup>33,34</sup> For example, MOFs containing strong metal-ligand bonds constructed from high valent metals such as Zr(IV), Hf(IV), and Cr(III) often demonstrate remarkable hydro-stability,<sup>35</sup> enabling them to be used for hydrogel applications. In addition, grafting long-chain molecules on the external surface of MOF particle was found to be effective for MOF kinetic stabilization in aqueous medium due to increased hydrophobicity.<sup>36</sup> For example, Xiao *et al.*, demonstrated that water-unstable HKUST-1 could be stabilized and used in biomedical application by incorporation of folic acid, through coordinative bonds, onto the coordinatively unsaturated metal sites present on the external surface of HKUST particles.<sup>37</sup> Moreover, Matzger and coworkers have shown that when monomers are grafted onto the MOFs for polymerisation, the resulting composite material becomes more hydrolytically stable due to support from the polymer.<sup>38</sup> Although this example was not a hydrogel, the organic polymer structure of hydrogels can be expected to similarly aid in stabilising MOFs. In addition, the large excess of water molecules can act as guests which fill the pores of the MOFs, reducing their intrinsic capacity for molecular adsorption and storage. Indeed, the storage capacity of MOFs can only be maximised when the pores are completely evacuated of competing guest molecules through activation.<sup>39</sup> Nonetheless, the flexibility of designing MOFs to vary the identities of the metal nodes, linkers and pore sizes has led to many innovative strategies for

achieving high drug loading, targeting and even controlled-release.<sup>40</sup> In fact, the confluence of the traditionally disparate fields of MOFs and hydrogels promises a vast design space for the optimisation of this class of composite materials, allowing a number of unique properties and performances to be achieved (Fig. 1).

In this review, we will discuss the current state-of-the-art and future possibilities of MOF-hydrogel composites as an important class of fourth-generation MOF material. After a summary of strategies to synthesise and characterise MOF-hydrogel composite materials, the most illuminating examples of MOF-hydrogels for applications in therapeutic payload delivery, biomedically-relevant sensing, materials for wound treatment and biocatalysis will be discussed. Wherever possible, we endeavour to highlight the unique properties conferred by this emerging class of hybrid materials, and possibilities offered by parallel developments in other areas of MOF research which are relevant for biomedical applications (e.g. therapeutic gas release). Finally, we conclude this review with our perspectives on how the field of MOF-hydrogel composites will evolve and the critical gaps in knowledge to be addressed for actual clinical applications to be realised.

## 2. Synthesis and characterisation of MOF–hydrogel composites

In MOF-hydrogel composites, MOFs can be considered as the dispersed phase with the bulk hydrogel material being the continuous phase.<sup>41</sup> Compared with strategies to prepare MOF-polymer hybrid materials,<sup>42</sup> methods for producing

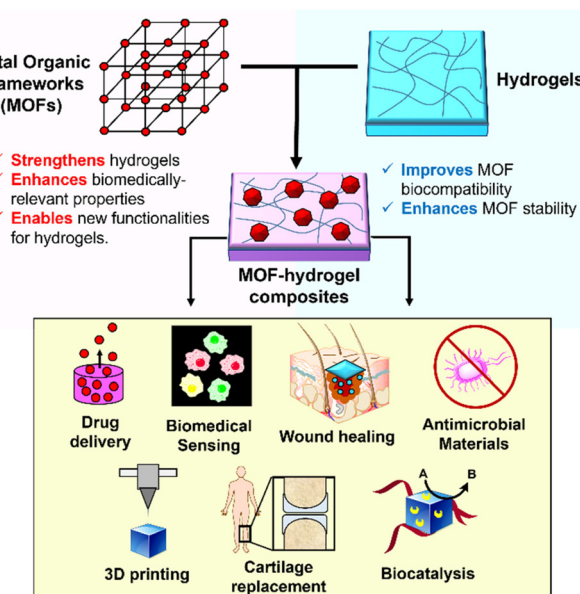


Fig. 1 Schematic illustration of how MOFs and hydrogels can complement each other in MOF–hydrogel composites, and their possible biomedical applications.



MOF-hydrogel composites are currently comparatively more limited. Indeed, considering that many hydrogels comprise of hydrophilic networks of polymers,<sup>43–45</sup> the methodologies for synthesising a diverse range of MOF–polymer architectures for different applications may be suitably adapted for MOF–hydrogels. The following describes common methods of synthesising MOF–thermogel composites.

## 2.1 Physical mixing of pre-synthesised MOFs to hydrogels

The most straightforward method to obtaining MOF–hydrogel hybrids is to simply add the pre-synthesized MOFs to the hydrogels. MOFs will have to be first synthesized *via* one of the many known methods in literature, such as through solvothermal, diffusion, microwave, electrochemical, mechanochemical and sonochemical means.<sup>46</sup> The solvothermal method of MOF synthesis is one of the most prevalent and is the conventional choice. The process involves first mixing up the precursors in a suitable solvent at a given temperature and pressure. In some instances, an autoclave is used and the reaction mixture is kept in a sealed vessel.<sup>47</sup>

The benefit of first making the MOFs is that there is vast literature describing many synthetic routes which can be tapped on to attain the MOF of interest. Moreover, the MOFs can be characterised and be directly used for comparative study with the hybrid MOF–hydrogel. Once the MOFs are successfully made, they are incorporated into hydrogels *via* several means. These include casting the MOFs directly onto the hydrogel,<sup>48</sup> mixing the MOFs into the hydrogel solution,<sup>49</sup> and adding the MOFs to a pre-polymer solution before polymerisation.<sup>32,50</sup> For instances where the MOFs are deliberately conjugated with the polymer, they will be described in section 2.2.

MOFs can be simply added to the pre-gel solution before it sets to form a hydrogel. This works across a wide variety of hydrogels including graphene hydrogel,<sup>51</sup> PLGA-PEG-PLGA,<sup>49</sup> and PVA.<sup>52</sup> In these cases, the MOFs are thoroughly stirred with the solution then ultrasonicated to remove bubbles and to ensure even dispersal. The way in which the gel is attained depends on the exact polymer used. With the amphiphilic PLGA-PEG-PLGA copolymer, the hydrogel is thermogelling,<sup>53</sup> *i.e.* exhibiting reversible sol–gel phase transition when warmed. In this case, the MOFs are added to a cold hydrogel solution and stirred before being set by bringing the mixture to a higher temperature beyond the gelation temperature.<sup>54</sup> Whereas for the graphene hydrogel, the carbonated ZIF-8 was added to a graphene oxide suspension and heated hydrothermally. Cooling to ambient conditions gave the required composite.<sup>51</sup> For physical MOF–hydrogel mixtures, non-covalent interactions such as hydrogen bonding, van der Waals interactions, and electrostatic interactions can occur on the interface between the polar MOF particles and polymers. However, the direct experimental observations of these interfacial interactions can be challenging, especially in the dispersed gel phase, though techniques such as FTIR can provide some insights. For example, the presence of 2D Ni–Fe MOFs in PVA resulted in red-shifts of the O–H FTIR stretch that was attributed to interfacial hydrogen bonding between both components

of the hydrogel.<sup>52</sup> The interfacial hydrogen bonding was also proposed to cause the structure of the 2D Ni–Fe MOF/PVA composite to become more compact. Separately, changes in the sol–gel transition of a PLGA-PEG-PLGA polymer solution in the presence of IRMOF-3 was proposed to result from hydrophobic interactions between the bridging organic linkers of the mOF and the PLGA segments of the polymer.<sup>49</sup>

Alternatively, the polymerisation process could take place after the MOFs are added. Liu *et al.*, came up with a strategy towards creating MOF–hydrogel hybrids. Different MOFs were added to a monomer solution of hydroxyethyl acrylate and acrylamide with an initiator.<sup>32</sup> Gelation then occurred with the MOFs present and interacting with polymer fibres in the hydrogel (Fig. 2). This synthetic strategy worked for ZIF-8, UiO-66 and ZIF-67. The MOFs were intended as nanofillers to toughen the hydrogels, and managed to impart superior mechanical stability and strength as expected. Interestingly, the MOF–hydrogel composites also showed better absorption capacity and longer release times for Rhodamine B. This was attributed to the hydrogel trapping and concentrating the cationic dye in the matrix, thus increasing the absorption by the MOF. Thus, MOF–hydrogel composites can be more suited for drug delivery when compared to the MOFs or hydrogels alone.

Interactions such as electrostatics and metal–ligand complexation are also effective means for MOF–hydrogel composite formation. For instance, MOF–hydrogels form when the negatively charged LAPONITE® nanoclay coats the surface of the ZIF-8 nanoparticles.<sup>55</sup> The work by Sutar *et al.*, showed that a hydrogel composite formed by coating of the ZIF-8 nanoparticles with LAPONITE® was able to enhance the thermal stability compared to the pristine MOF and allowed for better site-selective hydrogenation. Charge-assisted self-assembly was also achieved in a different system using carboxymethylcellulose (CMC) and MOF-5. Javanbakht *et al.*, showed that in presence of ferric chloride, the MOFs particles and Fe(III) irons can associate and form cross-links with CMC to give a composite without heating.<sup>56</sup> This biocompatible composite was used

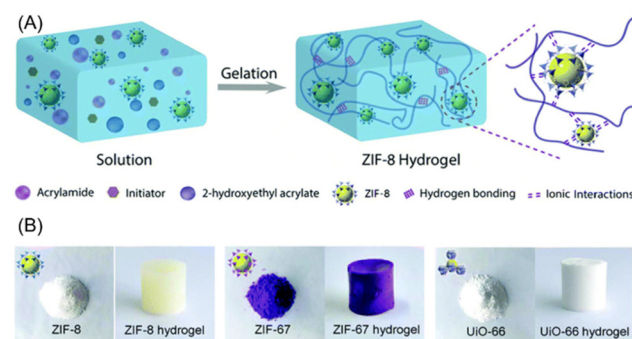


Fig. 2 (A) Synthetic strategy of adding the MOFs to a pre-polymer solution with the required monomers and initiators. Gelation gave the MOF–hydrogel hybrid. (B) The MOF powders and composite MOF–hydrogels as synthesized. Reproduced from ref. 32 with permission from the Royal Society of Chemistry, copyright 2019.



for delivery of 5-fluorouracil as an anti-cancer drug (details of this application in section 3.1).

## 2.2 Covalent conjugation of pre-synthesised MOFs with polymers

Covalent conjugation allows the formation of permanent cross-links between the pre-synthesised MOFs and the hydrogel polymeric network through reactive groups on both components. Alternatively, “bottom-up” modular approaches for synthesis of porous polymeric materials may be considered, using polymer-grafted metal organic polyhedral (MOPs) or cages (MOCs) that can be self-assembled into soft materials,<sup>57</sup> potentially including hydrogels. Covalent bond formation between radical crosslinking of unsaturated C=C bonds offer convenient and versatile means of chemical conjugation which can be easily-achieved under aqueous conditions. For example, Gwon *et al.*, employed the thiol-ene reaction to react the 4-arm thiolated PEG cross-linker with diacrylated PEG using UV photo-initiation to form a hydrogel encapsulating different MOFs<sup>50</sup> (Fig. 3). In this reaction, thiy radical formed from the thiolated-PEG propagates through the acrylate groups present, as well as the ethene moieties of the 1,2-bis(4-pyridyl) ethylene ligands of the MOFs to generate the photocrosslinked MOF-hydrogel composites which possessed antibacterial properties (Fig. 3).

Post-synthetic modification of MOFs is useful for appending reactive groups onto them for covalent grafting. This can

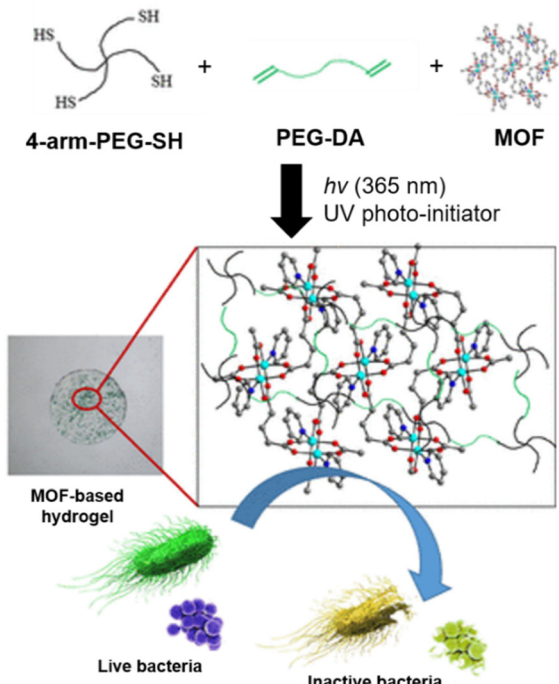
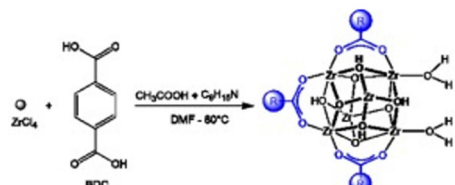


Fig. 3 Schematic of the subcomponents coming together in a UV initiated polymerisation with MOFs serving as cross-linkers in the composite. The resulting MOF–hydrogel was antibacterial. Adapted with permission from ref. 50. Copyright 2020 American Chemical Society.

be achieved by replacing the ligands on the MOFs with functional groups that can co-polymerise to link the MOFs to the polymer chain. For example, UiO-66 can be functionalised with acrylic acid *via* solvent-assisted ligand incorporation (SALI).<sup>58</sup> Arabic gum was also separately vinylated using glycidyl methacrylate. The MOF–hydrogel hybrid was then prepared by mixing with sodium persulfate to initiate the polymerisation.<sup>59</sup> The composite showed superior elasticity with its Young's modulus increasing by 535% and was superabsorbent. de Lima *et al.* also used a similar strategy with UiO-66 modified with acrylic acid, together with sodium alginate as the hydrogel.<sup>60</sup> The composite formed was used for drug delivery and showed good biocompatibility (Fig. 4).

(A) MOF synthesis



(B) SALI reaction



(C) HydroMOF reaction

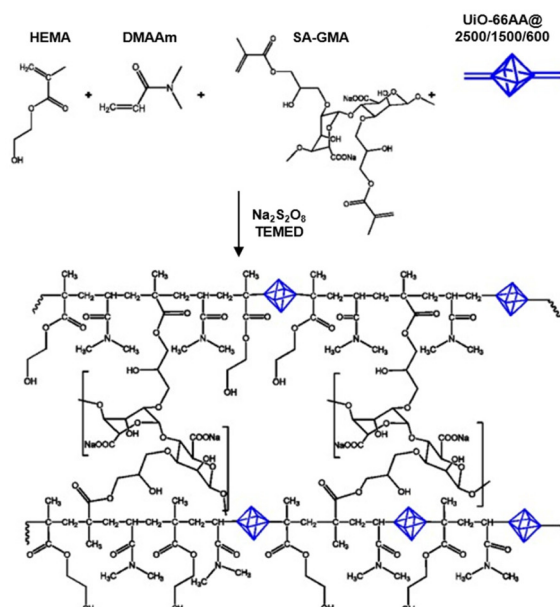


Fig. 4 Schematic showing the mechanism of the MOF–hydrogel. (a) Preparation of UiO-66 MOFs (b) Reaction of SALI in DMF to functionalise the UiO-66. (c) Formation of the hydroMOF using a radical polymerisation reaction. Reproduced with permission from ref. 60. Copyright 2021 Elsevier.

Biological components can also be incorporated to give MOF–hydrogel hybrids. Chen *et al.*, utilised crosslinked polyacrylamide chains functionalized with DNA hairpins using strand-induced hybridization chain reaction.<sup>61</sup> The azide functionalised nMOF was reacted with a nucleic acid hybridised dibenzocyclooctyne *via* click chemistry to functionalise the nMOF with nucleic acid. The DNA-polyacrylamide hydrogel was then used to coat the nMOF. The resulting composite was used in ATP-responsive drug delivery. This example demonstrates the innumerable ways in which the hydrogels can conjugate to MOFs. The cross-linking process need not be ionic or covalent; intermolecular hydrogen bonding interactions between DNA strands could facilitate the conjugation, and inclusion of biological components may in fact be beneficial for biomedical applications.

### 2.3 Growth of MOFs in hydrogels

In the earlier two methodologies described, the MOFs have to be prepared first before they are integrated with the hydrogels. To ensure even dispersion, many different strategies are employed. *In situ* growth of MOFs overcome this need to separately obtain the MOFs. The MOF–hydrogel hybrid can be obtained directly without any challenges that mixing or conjugation might bring. One of the earlier works in this methodology was reported by Zhu *et al.*, with an alginate-based composite.<sup>62</sup> The polymer solution was first added to a metal salt to give hydrogel beads. The metal-hydrogel beads were then added to the organic linker solution which allowed for *in situ* growth of the MOF (Fig. 5). This strategy worked for HKUST-1, ZIF-8, MIL-100(Fe), and ZIF-67, giving 4 different composites.

This methodology was similarly adapted for different hydrogel systems. For instance, Maan *et al.*, prepared ZIF-8 grown *in situ* on polyacrylamide hydrogels.<sup>63</sup> Klein and co-workers further improved upon the original method of *in situ* growth by using a green chemistry approach for the successful synthesis of Zr-containing MOF-808 particles using alginate.<sup>64</sup>

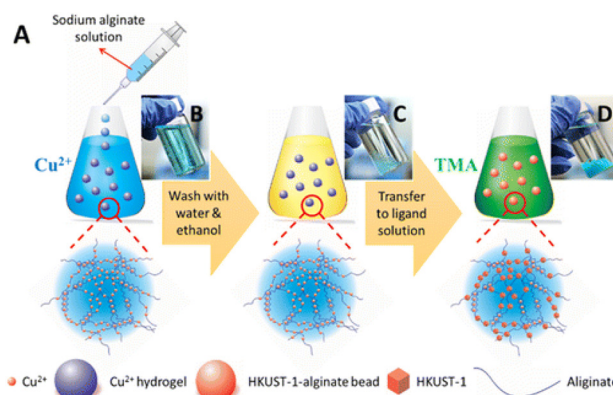


Fig. 5 (A) Schematic of the preparation of the MOF–alginate composite. Photographs of (B) alginate hydrogels cross-linked to  $\text{Cu}^{2+}$ , (C) alginate metal hydrogels after washing, (D) MOF–hydrogel hybrids. Reprinted with permission from ref. 62. Copyright 2016 American Chemical Society.

Water was used as a solvent and only moderate temperatures ( $50\text{ }^\circ\text{C}$ ) were required to make the Zr-based MOF–hydrogel hybrid. This is highly promising as these recent works illustrate the transferable nature of this methodology and its ease of use.

Instead of first incorporating the metal into the hydrogel, another strategy involves first dispersing the MOF ligand in the hydrogel. Liu and co-workers synthesised HKUST-1 in a 3D-printed double network hydrogel of acrylamide and alginate *via* *in situ* growth.<sup>65</sup> The precursor ink, consisting of acrylamide, cross-linker, photoinitiator, sodium alginate and MOF ligand was first printed and UV-cured to form a hydrogel matrix. Thereafter, the hydrogel was immersed into  $\text{Cu}(\text{NO}_3)_2$  solution for alginate cross-linking and *in situ* HKUST-1 synthesis to form composites with high MOF dispersity. These composites were highly stretchable and flexible, and could potentially be used across various applications for flexible materials.

More recently, this process was further streamlined into a single step preparation.<sup>66</sup> The metal salt, polymer and organic linker were mixed in a one-pot reaction in-bulk. Instead of growing the MOFs embedded within a pre-formed polymer matrix, this method relies on the direct growth of MOFs with simultaneous cross-linking of the alginate. A different integrated MOF–hydrogel was formed – instead of a smooth polymer framework with embedded MOFs, a MOF-like particulate structure was achieved. This composite designed by Zhuang *et al.*, had good regenerative properties and an adsorption capacity for tetracycline even greater than the on-surface MOF–hydrogel hybrid.

The MOF–hydrogels made *via* *in situ* MOF growth need not necessarily be the final product. In fact, as this method is rather streamlined, it is often used to make other MOF-containing materials of interest. Kong *et al.*, first made an alginate-graphene-ZIF-67 hydrogel *via* *in situ* growth before vacuum drying the MOF–hydrogel to obtain the corresponding aerogel.<sup>67</sup> Aerogels are rather similar to hydrogels except that the water molecules are removed and the pores of the MOFs are evacuated. In this case, the MOF–aerogel was utilised for tetracycline adsorption. MOF–hydrogels are also used to obtain MOFs embedded in hollow nanotubes or nanospheres.<sup>68,69</sup> The hydrogels serve as a good template for the growth of MOFs. Subsequent thermal decomposition of the hydrogels give rise to nanostructures of MOFs caging a target of interest. This shows the even greater opportunities that MOF–hydrogels can bring as intermediaries.

### 2.4 Characterisation of MOF–hydrogel composites

Given the diversity in methodology for synthesising MOF–hydrogels, there are also many different composite architectures that result. To verify that the composites are successfully made and to come up with an accurate representation of their structures, various characterisation techniques have to be used in tandem. Depending on the way that the MOF–hydrogels are made, each component can be separately characterised first. With MOFs, common techniques used include: scanning elec-



tron microscopy (SEM) and transmission electron microscopy (TEM) for visualisation of the structure and size, X-Ray Diffraction (XRD) to study the crystallinity of the MOF, adsorption studies (typically modelled with Langmuir or BET) to obtain surface area & pore volume, Fourier Transform-Infrared Spectroscopy (FT-IR) to verify functional groups of the organic linker and interfacial interactions between the MOFs and polymers, while Thermogravimetric Analysis (TGA) to study the thermal stability.<sup>70,71</sup> The methods are universally applied to study MOFs with different metal centres or organic linkers.

These techniques and the rationale behind using them can be extended to study the MOF-hydrogel hybrids. SEM is arguably the most commonly used technique when it comes to studying these hybrids, as it allows for clear visualisation of how the MOF particles embed onto the surface of the polymer fibres. In the work by Li *et al.*, SEM was able to illustrate the structures of the hydrogel, MOF and the combined composite (Fig. 6). Moreover, using the same instrument, Energy Dispersive X-ray Spectroscopy (EDX) can be performed to obtain the elemental distributions across the sample. In this case, it helped to verify the successful incorporation of N-doped graphene quantum dots onto the MOF-hydrogel hybrid.<sup>72</sup> In a separate study, SEM helped to elucidate the differences in structures obtained *via* a two-step *in situ* growth *versus* a one-step in-bulk *in situ* growth methodology described previously.<sup>66</sup> The SEM of the two-step method showed MOF particles embedded in a polymer matrix while the one-step

method led to an integrated MOF-hydrogel hybrid with more MOF-like structure.

SEM and EDX was similarly used by Maan *et al.*, to illustrate the successful synthesis of the MOF-hydrogel hybrid.<sup>63</sup> To further verify this, they performed extensive characterisation using the aforementioned techniques that are also often used for MOFs. TGA was used to determine the amount of ZIF-8 loaded. XRD showed that similar diffraction peaks were observed in the MOF-hydrogel and MOF but not in the pure hydrogel. FTIR showed that the composite possessed peaks from both the polymer backbone and organic linkers. Finally, X-ray Photoelectron Spectroscopy (XPS) was utilised to give an elemental analysis showing peaks in PAM and ZIF-8 both coming up in the composite (Fig. 7). Putting all these information together, there is strong supporting evidence and reason to believe that the composite material was successfully synthesised.

Further characterisation and studies will depend on the specific application of the MOF-hydrogel. For example, absorptivity and mechanical properties like tensile strength are studied for water filtration uses,<sup>59</sup> while cyclic voltammetry is used when the MOF-hydrogels are used as supercapacitors.<sup>72</sup> With biomedical applications, hydrogels and their MOF composites are often studied for water swelling, mechanical properties (rheological properties such as storage and elastic moduli, gel resilience and toughness),<sup>60</sup> biocompatibility (cell-studies), luminescence (UV-Vis absorption/fluorescence) for molecular sensing or bioimaging applications.<sup>73,74</sup> This will be dependent on the exact application of the composites and vary from study to study.

The characterisation of MOF-hydrogel composites has direct bearing on their performance for various biomedical

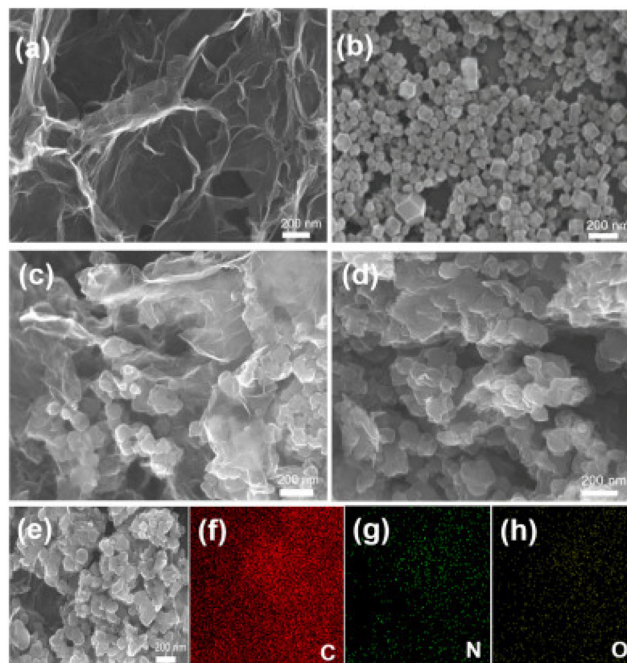


Fig. 6 SEM images of (a) Graphene hydrogel (b) cZIF-8 (c) MOF-hydrogel (d) Quantum dots on MOF-hydrogel. (e-h) Elemental mapping of the Quantum dots on MOF-hydrogel. Reproduced with permission from ref. 72. Copyright 2020 Elsevier.

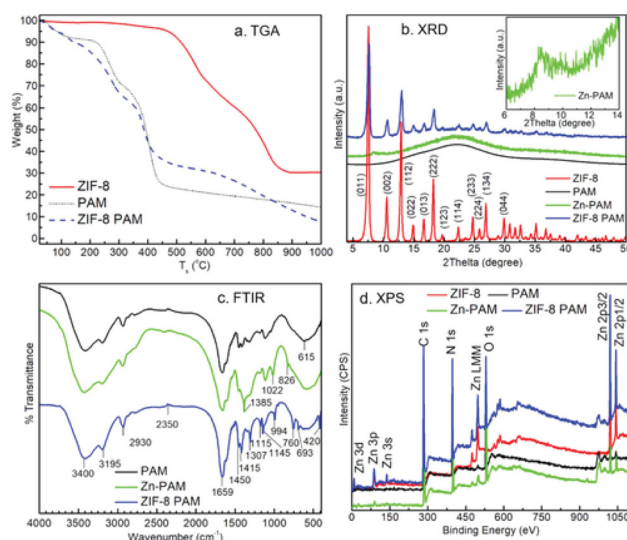


Fig. 7 Different characterisation methods used to provide support to the successful synthesis of ZIF-8/PAM hybrid. (a) TGA, (b) powder XRD, (c) FT-IR, (d) XPS. Reproduced from ref. 63 with permission from John Wiley and Sons, copyright 2019.



applications. For example, characterisation of MOF particle sizes through SEM imaging, and their dispersal throughout the hydrogel polymer matrix (by SEM imaging and EDX mapping) can greatly influence essential drug release parameters such as initial burst release, drug release rates and even the release mechanism.<sup>60</sup> In addition, studying the morphology of the composite materials through SEM imaging and characterisation of their degree of swelling gives indication of the network porosity and crosslinking density. These parameters influence the movement of water, solutes and analytes through the network for drug release and molecular sensing applications.<sup>74</sup>

### 3. Biomedical applications of MOF–hydrogel composites

As an important class of 4<sup>th</sup> generation MOF materials, MOF–hydrogel composites offer unique opportunities for biomedical applications which transcend those of their individual com-

ponents. To date, MOF–hydrogel composites have been applied to three major biomedical applications (Table 1), namely controlled release of therapeutic agents (section 3.1), sensing of biomedical agents (section 3.2), as hybrid materials for wound treatment (section 3.3) and for biocatalysis (section 3.4). Recently however, newer applications of MOF–hydrogels have emerged (section 3.5). In the following sections, we discuss the existing achievements and potential of MOF–hydrogel composites for various biomedical applications in greater detail.

#### 3.1 Controlled release of therapeutic payloads

Drug delivery agents are materials designed to release their therapeutic payload in a predictable manner over a period of time or upon demand. Not only would this reduce variability in the systemic levels of drugs, the reduced dosing frequencies will also lessen the socio-economic burdens to both the healthcare system and patients, whilst reducing drug wastage and any toxicity arising from drugs. In particular, the ability to deliver drugs to localised sites offers additional benefits of

**Table 1** Summary of recent advances in MOF–hydrogels for biomedical applications

Application	MOF–hydrogel	Brief details	Ref.
Controlled release of therapeutic payloads	IRMOF-3 + PLGA-PEG-PLGA	Thermogelling localised doxorubicin and celecoxib for oral cancer	49
	ZIF-8 + LAPONITE®nanoclay	pH sensitive release of fluorouracil	55
	MOF-5 + carboxymethylcellulose	Oral delivery of fluorouracil for colon cancer	56
	UiO-66 + alginate	Minimised burst release of prednisolone	60
	UiO-68 + polyacrylamide-DNA	ATP responsive release of doxorubicin for breast cancer	61
	MOF-5 + graphene oxide + carboxymethylcellulose	pH sensitive tetracycline release in gastrointestinal tract	75
	HKUST-1 + pectin/PEO	Electronspun mat for release of Cu and folic acid	76
	MIL-116(Ga) + alginate	Luminescent detection of chemotherapy drug mitoxantrone	74
	Eu-based MOF + Fe + alginate	Luminescent detection of penicillinase for allergy	77
	HKUST-1 + Au nanoparticles + DNA hydrogel	Ultrasensitive detection of adenosine	78
Sensing of biomedically-relevant agents	Cu-hemin MOF + glucose oxidase + agarose	Colorimetric detection of glucose	79
	UiO-66-NH <sub>2</sub> + agarose	Ratiometric detection of phosphate in serum	80
	Cu-TCP(Co) MOF + functionalised alginate	Signal amplified thrombin detection	81
	HKUST-1 + PPCN	Improvement of wound healing in diabetes using Cu	82
	Prussian blue nanoparticles + modified chitosan	Photo-responsive MOF–hydrogel with rapid bacteria trapping and killing	83
	bis(pyridyl)ethylene Co/Cu/Zn MOF + PEG	Antibacterial material for skin diseases	50
	ZIF-8 + PVA	Omniphobic wound dressing using Zn	84
	Vitamin-Cu/Zn MOF + alginate	Vitamin microfibres for wound healing	85
	Ag-based MOF + PVA/alginate/chitosan	Bilayer dressing with good haemostasis	86
	ZIF-8 + methacrylated hyaluronic acid	Antibacterial microneedle array that promotes wound healing	87
Materials for wound treatment	Enzymes encapsulated within agarose droplets stabilised by UiO-66 and magnetic nanoparticles, with ZIF-8 shell.	Catalysis of transesterification reactions	88
	Proteins and DNA on ZIF-8, ZIF-90, MarF-7 + hydrogels of melamine and salicylic acid	Tyrosine biosynthesis, enzyme-cascade reactions, cell-free protein synthesis	89
	Glucose oxidase (GOx) and horseradish peroxidase (HRP) on polyacrylamide + ZIF-8	Spatial organisation of incompatible enzymes for cascade reactions	90
	GOx&HRP@ZIF-8/polyacrylamide microparticles	Biocatalytic cascade reactions	91
	Ni–Fe based MOF + PVA	Cartilage replacement	92
Other emerging applications	ZIF-8 + polyurethane-gelatin	Bioink as matrix for 3D bioprinting	93
	Eu-UiO-67-bpy + gelatin methacryloyl hydrogel	Bioimaging agent for locating pulmonary nodules for potential early-stage cancer treatment	94



increasing their treatment efficacy and reducing side effects resulting from unnecessary systemic circulation. Other than the obvious requirement of biocompatibility, an ideal drug delivery agent should allow high drug loadings and controllable release rates. While organic systems such as hydrogels,<sup>30,44,95</sup> liposomes and micelles<sup>96–98</sup> are frequently used as drug delivery vehicles, problems such as burst release of drugs<sup>99,100</sup> and premature drug leakage are still often encountered.<sup>101</sup> Inorganic carriers such as mesoporous silica are often disadvantaged by their low drug loading capacity and comparatively difficult and limited opportunities for bottom-up pore engineering as compared with MOFs.<sup>15</sup> In 2006, the first application of MOFs (MIL-100 and MIL-101) for the delivery of ibuprofen, at a then-unprecedented drug loading capacity of 1.4 g of drug per g of MIL-101, was reported by Férey and coworkers.<sup>16</sup> In the decade since, there has been rapid development in the design and study of MOFs for drug delivery,<sup>102</sup> which also includes the use of hybrid materials such as MOF-hydrogel composites. Indeed, the amalgamation of MOFs and polymeric hydrogels have been shown to complement each other and bring about numerous unique advantages, as discussed below.

In drug delivery applications, the MOF-hydrogel is often intended for administration as a localised depot. Thus, it is key that the MOF-hydrogel is biocompatible and degradable. In many cases, natural polymers are utilised including cellulose and alginate.<sup>56,60</sup> Alternatively, other biocompatible polymers such as PEG or PLGA can also be used.<sup>54</sup> Hydrogels have high water content and mimic living tissues well<sup>27</sup> – making them excellent candidates to serve as reservoirs for drug delivery. However, in studies of drug release, hydrogels alone can be susceptible to burst release of drugs which could potentially lead to cytotoxicity. Inclusion of MOFs in the hydrogels has been shown to minimise this initial burst release and allow for a longer-term sustained release of the drug. For instance, de Lima *et al.*, showed that UiO-66 conjugated with alginate could lower the burst release of prednisolone.<sup>60</sup> This MOF-hydrogel hybrid was not cytotoxic, and when loaded with cytotoxic drugs, was able to slow the release sufficiently such that approximately 95% of the Vero cells tested remained viable after 24 h.

The converse is also true with hydrogels ensuring that the MOFs or drugs do not end up in systemic circulation. Extensive studies have been performed on using MOFs for drug delivery. Specifically, nMOFs are suitable with their high porosities allowing for large drug payloads.<sup>103</sup> However, not all MOFs are intrinsically biocompatible and may be toxic in circulation. Furthermore, certain drugs are intended for local application and would be harmful when systemic. Tan *et al.*, utilised IRMOF-3 in PLGA-PEG-PLGA thermogel to deliver doxorubicin and celecoxib locally for treatment of oral cancer. The benefit of this system is that the polymer exhibits a sol-gel transition. The drug & MOF can be mixed in with the polymer solution allowing for easy injection. Once in the body, the polymer gels up and ensures that the drug and MOF stays local (Fig. 8). This was studied *in vivo* and the drugs delivered

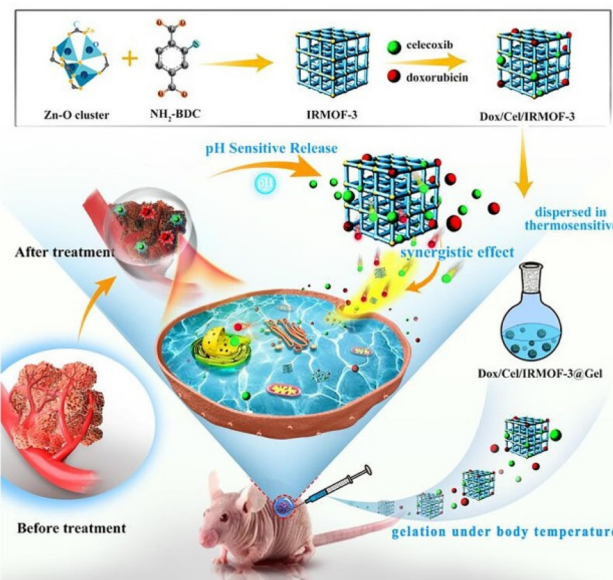


Fig. 8 Schematic showing the drug loaded-IRMOF-3 which is mixed with the thermogel for injection. Gelation occurs at body temperature to form a localised reservoir for drug release. Reproduced with permission from ref. 54. Copyright 2020 Elsevier.

induced tumour apoptosis and regulated angiogenesis.<sup>54</sup> Further studies showed that the composite had good biocompatibility with mitigated side effects from the toxicity of the MOF and drug.

The use of MOFs in hydrogels also allow for easy design and engineering of stimuli-responsiveness in drug delivery. While the equilibrium between drug encapsulation within the MOF pores and their liberation can be tuned by manipulating the host-guest intermolecular interactions from different functional groups<sup>104</sup> or pore sizes,<sup>105</sup> the ability to trigger the release of drugs on demand or on-site offers greater possibilities for targeted delivery. A number of MOFs that can release their therapeutic payloads either upon chemical (e.g. pH change, presence of specific molecules) or physical stimuli (e.g. light, temperature, sonication) have been designed.<sup>106,107</sup> For instance, a popular strategy involves the triggered release of “molecular gatekeepers” that cap the external surface of MOFs by breaking the covalent bonds or supramolecular host-guest inclusion complexes (e.g. with cyclodextrin and pillarenes) using pH, temperature or light. This opens the pores of the MOFs, thereby liberating their encapsulated drugs.<sup>108,109</sup> Temperature can be used to modulate the framework structure, triggering a conversion from a closed to an open phase that allows payload release.<sup>105</sup> Indeed, the many possibilities of engineering responsiveness<sup>45</sup> can allow design of specific MOF-hydrogel composites targeted for any biological context.

There are several examples of MOF-hydrogels showing a pH-sensitive response. For instance, certain MOFs are stable under neutral conditions but may degrade when exposed to acid.<sup>33</sup> This property is exploited by Chakraborty *et al.*, using ZIF-8 & LAPONITE® composite. This composite is stable under



neutral conditions but decomposes when the pH drops.<sup>55</sup> This allows for the targeted release of fluorouracil within the more acidic tumour microenvironment.<sup>110</sup> The use of pH stimuli is also useful for the delivery of drug to specific regions of the gastrointestinal (GI) tract. The stomach has a more acidic pH than the intestines. Coating the drug embedded-MOFs with anionic carboxymethylcellulose (CMC) can protect it against the stomach pH. This allows a more sustained release later in the GI tract. The pH sensitive nature of MOF-CMC hybrids was used to deliver anti-cancer drugs and antibiotics in a more localised manner.<sup>56,75</sup> The drug release studies in both cases showed that the MOF-hydrogel hybrid had better performance compared to the MOF alone. This controlled release allows for oral delivery of the drug instead of other more invasive methodologies.

Another type of stimuli sensitivity is shown in the study performed by Chen *et al.*, with a DNA-polyacrylamide hydrogel with UiO-68 (synthesis discussed in section 2.2).<sup>61</sup> The polyacrylamide is functionalised with DNA hairpins and forms a hydrogel around the UiO-68. In high ATP concentrations, the drug carried by the composite is triggered to release. One of the emerging hallmarks of cancer is the reprogramming of metabolism to meet the needs of rapid cell proliferation,<sup>111</sup> thus the tumour microenvironment is richer in ATP. Exploiting this property of tumours, this DNA-polyacrylamide hydrogel allows for specific release of doxorubicin to these sites. This example highlights the tunability of the composite and how it can be designed to be specific to certain stimuli for controlled release.

While in previous examples the MOF either encapsulates a therapeutic agent or has drug-precursors covalently built into its linkers, there need not always be a drug that is carried by the MOF. The active agent can in fact be the metal ions that leach out of the MOF-hydrogel composite. This is illustrated in the work by Kiadeh *et al.*, where a Cu-based MOF containing folic acid (vitamin B9) was embedded in pectin. The MOF-hydrogel was bactericidal when tested with *E. coli* and *S. aureus*. Besides being a system for drug delivery, this composite also had potential to be used for wound healing.<sup>76</sup> Further examples of composites used for wound healing will be discussed in section 3.3.

**3.1.1 Therapeutic gas delivery.** In addition to small molecule drugs and biologics, the ability of a number of gases (*e.g.* NO, O<sub>2</sub>, CO, H<sub>2</sub>S, Xe) to elicit beneficial biological responses for disease treatment is gaining popularity in recent years.<sup>112</sup> For example, nitric oxide (NO) plays important roles in human biology, such as being neurotransmitters and neuromodulators in the human central nervous system,<sup>113–115</sup> and is now accepted as a treatment for pulmonary hypertension due to its ability to relax vascular smooth muscle.<sup>116</sup> Like NO, carbon monoxide (CO) is a gasotransmitter, as well as possessing anti-inflammatory and anti-apoptotic properties.<sup>117</sup> Even Xe, despite being an inert gas, can elicit notable biological responses that can potentially be used for neuroprotection against traumatic brain injury or stroke.<sup>118</sup>

Compared to classical drugs, therapeutic gases are much smaller and thus are able to rapidly diffuse across membranes

and even the blood-brain barrier. Despite their therapeutic benefits, these gases also possess systemic toxicities, making the ability to control their dosage, location and duration of release of paramount importance. Traditionally, delivery of therapeutic gases can be achieved using liposomes or microbubbles, but these delivery vehicles offer little opportunities for stimuli-responsive release other than *via* acoustic cavitation.<sup>119</sup> Furthermore, they have limited gas carriage capacities, with liposomes able to carry up to 10% gas by volume.<sup>120</sup>

With their intrinsically high gas storage capacities and possibilities for built-in field-responsiveness (a key feature of 3<sup>rd</sup> generation MOFs) that allow on-demand, stimuli-triggered gas release, MOFs offer unique potential as vehicles for spatio-temporal delivery of therapeutic gases. A number of notable examples have been reported in recent years. For example, nitro-imidazole linkers can be used to construct stable and robust ZIF structures that can undergo photo-induced nitro-to-nitrite rearrangement and subsequent bond cleavage to release NO.<sup>121</sup> These MOFs can allow NO delivery at precise sites at the cellular level by localised laser activation. In another example, photo-triggered NO release was accomplished from photo-active *N*-nitrosamine functional groups.<sup>122</sup> In both examples, the MOFs showed better photoactivity than the individual uncoordinated linkers, due to the porous structures enforcing linker segregation that prevents quenching of reactive excited states. Photoresponsive delivery of CO from MOFs was also reported using a manganese-carbonyl complex immobilised onto the organic linker of robust Zr(IV)-containing MOFs, using low intensity light as a trigger.<sup>123</sup> While MOFs for stimuli-responsive gas delivery are currently not yet demonstrated in hydrogel composites, the innovative strategies outlined here potentially can be applied immediately for the hybrid materials, which can confer benefits such as improved biocompatibility and can potentially further modulate gas release and delivery.

### 3.2 Sensing of biomedically-relevant agents

The tunability of MOFs, high internal surface areas and their ability to specifically bind target guests make them especially suited for sensing applications.<sup>11</sup> Towards this end, luminescent MOFs are especially useful due to their sensitivity for specific analyte detection, exploiting their ability to modulate the numerous emissive phenomena possible. A number of mechanisms underlying luminescent behaviour in MOFs have been elucidated. Other than emissive linkers containing organic lumophores (*e.g.* pyrene, anthracene, naphthalenediimide),<sup>124–126</sup> the metal nodes can also contain luminescent lanthanide cations such as Eu<sup>3+</sup> and Tb<sup>3+</sup>. In addition, luminescence can also arise from energy transfer mechanisms such as ligand-to-metal charge transfer (LMCT), metal-to-ligand charge transfers (MLCT), antenna effects and formation of excimers.<sup>127</sup> These varied mechanisms enable their exploitation to detect and monitor different substances and their concentrations in organisms, potentially allowing disease diagnosis, metabolite monitoring and even elucidation of different pathological mechanisms. However, crystalline



MOF powders can suffer from poor stability in biological media, and can be easily dispersed from their sites of application, which leads to wastage and loss of detection sensitivity.

Hydrogels which are biocompatible can serve as an excellent matrix to hold the MOF sensors. The composite MOF-hydrogel can also be potentially reusable as the MOFs are not dispersed away. Lian *et al.*, made a mixed matrix membrane (MMM) comprising Eu@MIL-116(Ga) in an alginate hydrogel. Post-synthetic metalation of MIL-116 with Eu<sup>3+</sup> ions did not disrupt the structure of the MOF. Under UV irradiation, the Eu embedded in the MOF hydrogel fluoresces. In the presence of mitoxantrone, quenching of this fluorescence is observed. This system could achieve parts-per-billion sensing sensitivity, with excellent selectivity as other chemicals commonly found in serum did not induce a similar order of magnitude in quenching. Moreover, the composite can be used to coat fabrics or paper which allows for ease of use and recyclability.<sup>74</sup>

Another system developed by Lian & Yan also utilised Eu as the source of luminescence. However, instead of metalating another MOF with Eu<sup>3+</sup>, this study employed the use of an Eu-based MOF synthesized hydrothermally.<sup>77</sup> In this application, beyond serving as a matrix for the MOF, the hydrogel also contains embedded Fe<sup>3+</sup> ions which help with binding of penicillamine. Penicillamine is the metabolic product of penicillin, and its presence indicates that the serum contains  $\beta$ -lactamases. Without sufficient  $\beta$ -lactamase, there will be an accumulation of penicillin which likely leads to an allergic response. The MOF-hydrogel composite allows for incorporation of other elements that can complement detection of the target of interest. This cannot be achieved by just utilising MOFs in the powdered form.

With MOF-polymer hybrids, it has been shown that the polymer can in fact help in stabilising the MOF.<sup>38</sup> Similarly, hydrogels can also provide added stability to the MOF. Several MOFs have been shown to be effective for phosphate detection.<sup>128,129</sup> However, in some of these cases, the MOFs tended to collapse and cannot be reused while in other cases, it has not been shown to work in a biological serum. Gao *et al.*, developed a system using RhB@UiO-66-NH<sub>2</sub> immobilised in an agarose gel which could successfully detect phosphate in serum. This composite was stable and could avoid interference caused by other chemicals commonly found in serum. In addition, this is a fluorescent system that allows for identification of phosphate presence with the naked eye.<sup>80</sup> The greatest benefit of using a composite was that the phosphates can be removed when flushed with Eu<sup>3+</sup> solution which allows for the composite to be reused. This can only be achieved if the MOFs do not degrade and are not removed in the process.

In the presence of target guest molecules, certain MOF-hydrogels can also release the MOF itself to trigger optical and/or rheological responses. Lin *et al.*, designed a system where the Au@HKUST-1 was released in presence of adenosine which led to the dissolution of the DNA hydrogel.<sup>78</sup> The released MOF had peroxidase-like activity which catalysed a chemiluminescent response in presence of luminol and hydro-

gen peroxide. In another instance where alginate is used as the hydrogel, the MOF was released in presence of thrombin and also led to a chemiluminescent response.<sup>81</sup> In both cases, aptamers were used to achieve biological stimuli sensitivity. The hydrogels were needed to hold the MOFs in place and only allow for a response in presence of the stimuli. These examples further underscore how the tunability of MOF-hydrogels and the variety of strategies allow for a biologically appropriate system to be developed.

While many of the strategies utilised luminescence as a means for ease of detection, colorimetric methods are also possible. Lin *et al.*, first showed that glucose oxidase with Cu-hemin (GOD@Cu-hemin) MOF was a suitable bienzymatic catalyst that was more stable than free peroxidase. When embedded together with 3,3',5,5'-tetramethylbenzidine (TMB) in an agarose gel, the hybrid hydrogel can differentiate glucose concentrations based solely on colour (Fig. 9).<sup>79</sup> The peroxide generated during the reaction catalysed by GOD@Cu-hemin oxidises the TMB, which leads to the colour observed. Indeed, these aforementioned studies show the diversity of methods by which MOF-hydrogels can be used for detection and selective sensing of molecular targets, by incorporating different sensing elements within the MOF and hydrogel components of the composites.

### 3.3 Materials for wound treatment

For a material to be suitable as a dressing for wound healing, the most important criterion is that it is not cytotoxic and is biocompatible. Metal ions such as copper are long known to be helpful in inducing angiogenesis and in promoting wound healing.<sup>130</sup> However, the concentrations of these metal ions are also important<sup>131</sup> and large excesses might end up being toxic to the host cells. Thus, direct application of copper MOFs to wounds could potentially lead to adverse effects. MOF-hydrogels prevent such effects by controlling and sustaining the release of the bioactive copper cations. Xiao *et al.*, made a composite consisting of HKUST-1 nanoparticles in an antioxidant and resorbable citrate-based hydrogel.<sup>82</sup> Other than

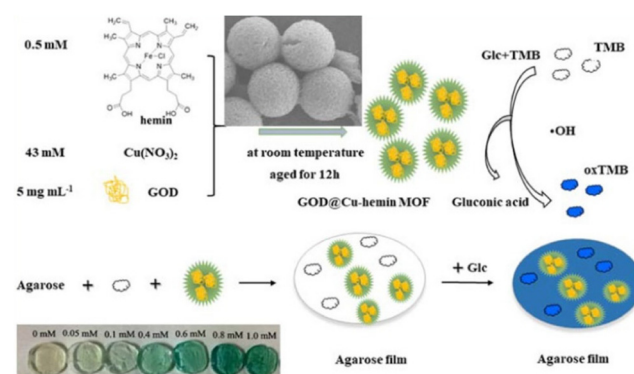


Fig. 9 Schematic of the peroxidase-like activity of the MOF and how the MOF-hydrogel film can be used to detect different concentrations of glucose by colorimetry. Reproduced with permission from ref. 69. Copyright 2021 Elsevier.



slowing down the release of copper cations, the hydrogel also aided in ensuring that the MOF does not degrade too quickly. When tested *in vivo*, this composite was able to induce angiogenesis and promote re-epithelialization. In a separate example, Yu *et al.*, made microfibres with a vitamin-based MOF core surrounded by an alginate shell. The composition of these fibres, such as their thickness, can be adjusted to control the amount of metal ions released.<sup>85</sup> The hybrid material consisting of both zinc- and copper-based cores showed fastest wound healing and closure (Fig. 10). Beyond promoting wound healing, the dressing would also benefit from being bactericidal. The vitamin-laden microfibres were tested and shown to decrease *E. coli* count.

In other instances, the MOF-hydrogels are specifically designed to be antimicrobial in nature. Gwon *et al.*, made photo-crosslinked hydrogels with different metal-based MOFs and tested them against *E. coli* and *S. aureus*. Both the Co- and Cu-based MOFs and their corresponding hydrogel composites showed good bactericidal activity. The Cu-based MOF was further shown to have no cytotoxicity towards human dermal fibroblasts.<sup>50</sup> While the composite was not tested for its wound healing ability, Cu(II) ions, which are released slowly from the composite in saline solution, are known to stimulate angiogenesis and enhance wound healing. Yao *et al.*, developed a ZIF-8 in PVA composite that was intrinsically hydrophilic while being omniphobic on the surface. This hydrogel is dual purpose as it not only benefits from being able to contain

and release bactericidal agents, but also prevents bacteria from adhering to the material.<sup>84</sup> In addition, the zinc ions are also anti-inflammatory and promote healing. These examples elucidate the suitability of MOF-hydrogels as a sterile dressing that can additionally stimulate faster recovery.

The flexibility in which the MOF-hydrogels can be prepared allows for many novel dressings that can further improve on these properties. Microneedles are a painless and minimally invasive method to introduce active agents transdermally or intra-dermally.<sup>132</sup> Yao *et al.*, has demonstrated that MOF-hydrogels fabricated into a microneedle array was able to greatly accelerate epithelial regeneration and neovascularisation.<sup>87</sup> The ZIF-8 particles in the methacrylated hyaluronic acid (HA) hydrogel slowly released zinc ions which were bactericidal and HA which promoted wound healing.<sup>87</sup> The composite when made into such an array was able to penetrate deeper to release these active agents (Fig. 11). Another novel idea was illustrated by Zhang *et al.* with a bilayer dressing. The upper layer contained Ag-based MOF with chitosan nanoparticles while the lower layer contained PVA/alginate/chitosan. Although the upper layer was not biocompatible, it has good bactericidal activity. Meanwhile, the lower layer, was biocompatible and will be in direct contact with the wound. Moreover, the lower layer could promote blood coagulation and cell proliferation.<sup>86</sup> The inherent tunability of MOF-hydrogels with regards to their structure and composition permits these innovative advances.

### 3.4. Biocatalysis

Biocatalysis is also an important target of MOF-hydrogel composites as both MOFs and hydrogels can work as catalyst support. In addition, MOFs can chemically and mechanically stabilize the hydrogel, and can prevent catalyst leaching from the hydrogel. Thus, recently, MOF-hydrogel composites show significant potential in various biomedical applications including biopharmaceuticals, tandem chemoenzymatic catalysis, and biodegradation media.<sup>133</sup>

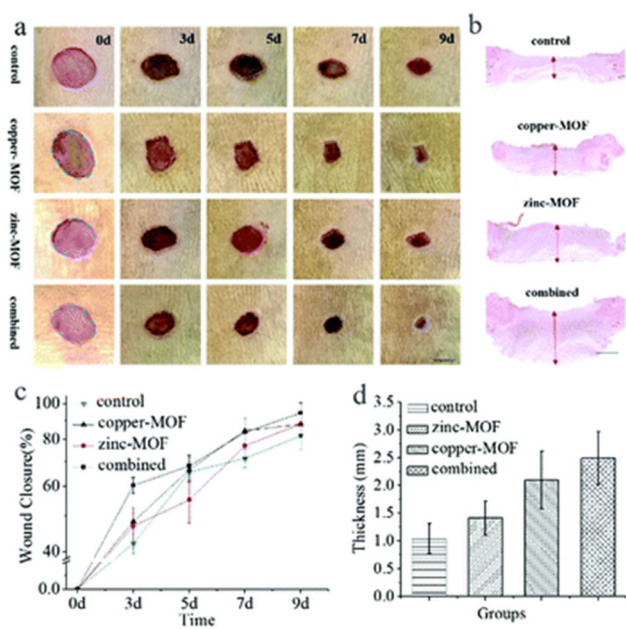


**Fig. 10** Figure Caption. Effect of MOF-hydrogel microfibres on wound healing. (a) Photos of skin wounds treated with control, copper-MOF microfibres, zinc-MOF microfibres, and combined MOF microfibres. (b) H&E staining of the wounds after 9 days at low magnification. (c) Statistical graph of wound closure. (d) Quantitative analysis of granulation tissue thickness. Reproduced from ref. 85 with permission from the Royal Society of Chemistry, copyright 2018.

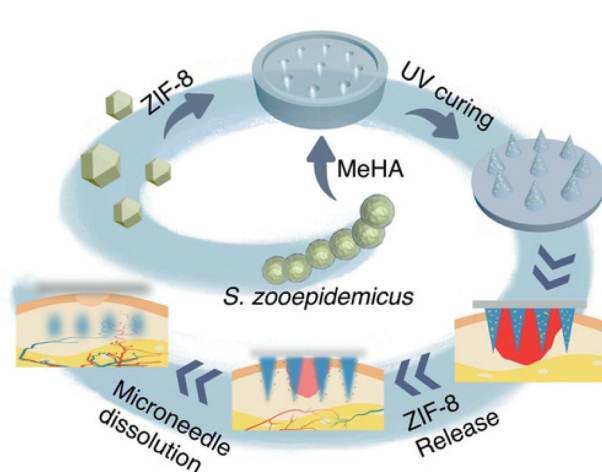


**Fig. 11** Schematic illustration of the microneedle array MOF-hydrogel composite used in promoting wound healing. Reproduced from ref. 87 with permission from John Wiley and Sons, copyright 2021.



Huo *et al.*, synthesised an agarose hydrogel droplet stabilized with UiO-66 and magnetite nanoparticle as a template around which to form a hierarchically structured ZIF-8.<sup>88</sup> The resulting MOF–hydrogel composites were highly microporous and were easily recovered by a magnet owing to the incorporated magnetite. The MOF–hydrogel composites contained hydrogel core, which can encapsulate several large biomolecules such as green fluorescent protein (GFP) or fluorescein isothiocyanate (FITC)-tagged enzymes *Candida Antarctica* lipase B (CalB) and *b*-galactosidase (*b*-gal). The enzyme loaded MOF–hydrogels maintained a high degree of porosity which indicated the enzyme immobilization in the hydrogel core. The CAL-B immobilized MOF–hydrogel exhibited catalytic activity toward transesterification reaction comparable to the free enzymes. Moreover, they exhibit good recyclability and size-selectivity.

Wenyan *et al.*, reported the highly efficient immobilization of various biomacromolecules on MOF–hydrogel composites *via* simple mixing of the biomolecule, and hydrogels of melamine and salicylic acid, and MOF precursors.<sup>89</sup> Specifically, typical MOF materials, ZIF-8, ZIF-90, MarF-7 were chosen as the support materials. Moreover, the catalytic performance of the enzyme-immobilized MOF–hydrogels could be fine-tuned by controlling the size of the MOF–hydrogels by introducing different quantities of hydrogel. Yuhao *et al.*, first demonstrated the biomimetic cascade catalysis using MOF–hydrogel composite consisting of polyacrylamide (pAAm) hydrogel microsphere covered by ZIF-8.<sup>90</sup> They realized a competitive cascade enzymatic reaction by immobilizing glucose oxidase (GOx) and horseradish peroxidase (HRP) in the inner pAAm microsphere while immobilizing catalase (CAT) in the outer ZIF-8 layer. The hybrid multi-component reactor performed incompatible enzyme reactions to give discrete reaction fluxes and product outputs, as occurring in natural cells. Recently, Zhang *et al.*, developed a simple and efficient strategy to create multi-enzyme-loaded MOF–hydrogel composite (GOx&HRP@ZIF-8/polyacrylamide) microparticles, for biocatalytic cascade reactions by the utilization of droplet microfluidic techniques.<sup>91</sup> Uniform polyacrylamide precursor droplets formed by microfluidics, which contain ZIF-8 particle incorporating cascade enzymes, were used as templates to create the hydrogel microparticles. The resulting MOF–hydrogel composite microparticles exhibited enhanced stability for the cascade reaction after treatment in harsh conditions, as well as good recyclability. This preparation technique have high potential for multi-enzyme immobilization with enhanced stability and reusability for various biocatalytic cascades.

### 3.5. Other applications

Many of the aforementioned applications of MOF–hydrogels exploited the intrinsic properties of MOFs, such as porosity which allowed for binding of specific drugs or luminescent agents. However, MOFs can also serve as fillers in hydrogels to improve their mechanical properties. For example, Gao *et al.*, showed that 2D Ni–Fe MOF sheets raised the tensile strength

of the PVA hydrogel, allowing the composite material to be utilised as an anti-wear cartilage replacement.<sup>92</sup>

Similarly, when ZIF-8 was introduced into a gelatin–polyurethane hydrogel bio-ink, the material showed improvements in its printability and shear-thinning ability. This allowed for the material to be better suited for 3D bioprinting. Despite this, the concentration of ZIF-8 in the composite was too high for the material to be biocompatible.<sup>93</sup> In another example, a 3D-printed double network hydrogel of acrylamide and alginate, containing HKUST-1 synthesised *in situ*, demonstrated high strength, stretchability and toughness.<sup>65</sup> The mechanical properties of the 3D-printed MOF–hydrogel composite could be easily tuned by varying their composition and printing parameters, and could be used to print 3D shapes of varying complexities, including dumbbells, pyramids and grids. These 3D printed composites have the potential for creating high-resolution 3D structures for fabrication of biomedical devices, wearables and flexible sensors.

Inspired by the promising uses of MOFs for bioimaging demonstrated in recent years,<sup>134</sup> applications of MOF–hydrogel composites for this application are gaining interest. Recently, the Eu–UiO-67-bpy MOF (bpy = 2,2'-bipyridyl) was used as a fluorescent dye embedded within a gelatin methacryloyl (GelMA) hydrogel matrix to improve the localisation of pulmonary nodules (Fig. 12).<sup>94</sup> These nodules are small lesions (diameters < 1 cm) and are related to early-stage lung cancer, thus they are receiving interest for early diagnosis.<sup>135</sup> However, these nodules are often invisible during surgery, making their localisation challenging, and existing preoperative tumour marking techniques (*e.g.* hookwires) are invasive.<sup>136</sup> In this study, the authors demonstrated that Eu–UiO-67-bpy showed stable red luminescence under UV excitation, and could also be used in CT imaging as the MOFs efficiently absorbed X-rays. The GelMA hydrogel not only improved the MOF's biocompatibility by restricting its release into the surrounding tissues, but also provided suitable viscosity for injection through small needles. Furthermore, the presence of gel provided palpability for the injection site that facilitates nodule detection. Although this MOF–hydrogel composite can

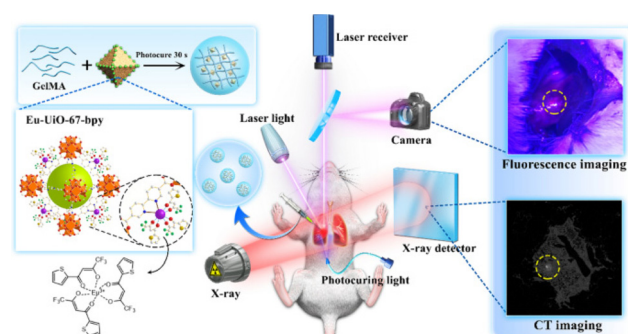


Fig. 12 Eu–UiO-67-bpy/GelMA MOF–hydrogel composites for locating pulmonary nodules through fluorescence–CT dual-modal imaging. Figure reproduced from ref. 94. This article is licensed under a Creative Commons Attribution 4.0 International License.



improve the accuracy of locating and excising these nodules, the use of UV light can be damaging to tissues, and the red luminescence of  $\text{Eu}^{3+}$  may not provide sufficient contrast from the red coloration of the surrounding tissues and blood. Future developments in this novel application space will be highly anticipated.

## 4. Conclusions and outlook

In conclusion, our survey of MOF-hydrogels hybrids has demonstrated that the unity of the traditionally disparate fields of MOFs and hydrogels offered immense potential for designing a new class of composite biomaterials, marrying the properties of both materials to great effect. This was seen with composites where the MOF and hydrogel play different roles in biomedical sensing<sup>77,78</sup> and promoting wound healing.<sup>86,87</sup> Furthermore, both components can also complement each other and mitigate the other's shortcomings, evident from the ability of MOFs to strengthen hydrogels<sup>93,137</sup> and prolong the sustained release of drugs from the composites.<sup>60</sup> Likewise, hydrogels can improve the biocompatibility<sup>54</sup> and stability of MOFs under biological conditions.<sup>56,75</sup> Their great diversity and tunability permits many innovative concepts to be adapted into a biomedical context, as illustrated by how DNA aptamers can give rise to stimuli-responsiveness.<sup>61,78,81</sup> Nonetheless, despite the recent exciting advances in biomedical applications discussed in this review, as well as in other promising use cases such as for water remediation,<sup>138,139</sup> the field of MOF-hydrogel composites is still in its infancy, with its immense potential yet to be realised.

With growing interest in this hybrid material, synthetic strategies towards making MOF-hydrogels are also improving in both ease and structural diversity. This review covered some of the broader methodologies used, namely adding MOFs to hydrogels,<sup>32,48,50,54</sup> chemically conjugating MOFs with hydrogels<sup>55,56,59,60,83</sup> and *in situ* MOF formation in hydrogels. Characterisation of these materials showed the variety in architectures which can be achieved, be it polymer-like<sup>62</sup> or MOF-like<sup>66</sup> structures, enabling design-driven synthesis of MOF-hydrogel hybrids for various applications. This review focused on the biomedical applications of MOF-hydrogels but also included several examples of synthetic strategies used to make MOF-hydrogels for other purposes; these composites can potentially be adapted for biomedical uses as well. Recent advances depict the future promises that this hybrid material can deliver, such as in 3D bioprinting<sup>65,93</sup> for wearables and implants, and we believe that there will be many more innovative and valuable use-cases in the near future.

MOF-hydrogel composite materials are poised to offer many new and highly-desirable treatment modalities difficult to achieve using hydrogel materials alone. As aforementioned, the MOF-hydrogel composites can allow dose-control or stimuli-responsive release of therapeutic gases. Alternatively, instead of achieving the desired therapeutic effects by drug delivery, newer treatment strategies can be explored using

MOF-hydrogel composites. For instance, microwave dynamic therapy can be combined with microwave thermal therapy using Mn-doped zirconium MOF nanocubes<sup>140</sup> to achieve simultaneous reactive oxygen species (ROS) and heat generation to suppress tumour growth. The use of MOFs with porphyrin scaffolds<sup>141</sup> in hydrogel formulations can also potentially allow visible-light promoted ROS generation for antimicrobial applications. These can potentially be beneficial over antimicrobial MOF-hydrogel formulations that work based on controlled release of agents such as  $\text{Ag}^+$ , whose antimicrobial effects are lost as soon as the reservoir of agents are depleted. In addition, MOF-hydrogel composites can offer convenient means of device fabrication for sensitive and rapid detection and sensing of gaseous biomarkers (e.g.  $\text{H}_2\text{S}$  for asthma diagnosis<sup>142</sup>) and even bacteria.<sup>143,144</sup>

The highly-promising and exciting developments already achieved on the lab scale in this nascent field offer great potential for MOF-hydrogel composites to find actual real-life biomedical applications over a longer horizon. In this respect, there are several critical challenges to be addressed. Most critically, the biological tolerance to MOFs of diverse architectures (organic linkers + metal nodes) still remain an unanswered question. Thus far, studies evaluating the cytotoxicity of MOF materials are limited to short-term *in vitro/in vivo* acute toxicity experiments. Even in the form of a composite hydrogel made up of biocompatible polymers, the long-term toxicity of MOFs, with regards to accumulation in tissues, need to be studied, especially for *in vivo* applications.<sup>145</sup> *In vivo* natural biodegradation pathways of MOFs and their hydrogel components also need to be elucidated, including their bio-distribution, metabolism and eventual excretion. Nonetheless, potential toxicity and immunogenicity issues can be possibly minimised by the use of biocompatible metals such as Ca, Mg, Fe and Zn as metal nodes for the MOFs,<sup>146</sup> and/or endogenous molecules as linkers in these composite biomaterials. The demonstrated feasibility of synthesising stable MOFs from naturally-occurring bio-ligands such as peptides, amino acids, nucleobases and saccharides,<sup>147</sup> as well as their proven usage in drug delivery<sup>148</sup> and molecular sensing<sup>149</sup> offer excellent promise.

Finally, the practicalities of scale-up MOF-hydrogel composite synthesis and clinical translations should be examined. Although the field is still nascent, we believe that a thorough consideration of these practicalities at an early stage will prove invaluable in future translations of promising MOF-hydrogel composites. Indeed, large-scale syntheses of MOFs alone remain an ongoing challenge, with processes such as post-synthetic removal of impurities from MOFs and the subsequent activation presenting considerable difficulties on large scales.<sup>150</sup> In a similar vein, scale-up syntheses of MOF-hydrogel composites should ideally be economical and sustainable, avoiding the use of large quantities of toxic solvents such as DMF which are commonly used for lab-scale MOF syntheses. Manufacturing of MOF-hydrogel composites also need to be compatible with current good manufacturing practices (cGMPs), which can already pose considerable hurdles for biomaterials-based hydrogels by themselves.<sup>151</sup> Critical para-



meters which need to be assessed include batch variations and reproducibility, safety, robustness and reaction efficiency. The use of natural polymers such as alginates, commonly used in MOF-hydrogel composites, may face additional challenges owing to their natural heterogeneity and impact batch-to-batch consistencies. Lastly, sterilisation and optimal storage conditions of MOF-hydrogel composites will eventually need to be evaluated as well. Despite these considerable challenges, we are confident that as the field matures, many exciting and innovative solutions will be developed in coming years to address these issues. We anticipate many exciting developments in the years to come.

## Conflicts of interest

There are no conflicts to declare.

## Acknowledgements

S. K. is grateful for the support from Kyoto University's Overseas On-site Laboratory Program, and the financial support of KAKENHI, Grant-in-Aid for Scientific Research (S) (JP22H05005); J. Y. C. L. and X. J. L. acknowledges the IAF-PP grant (OrBiTAL: Ocular Biomaterials for Vitreoretinal Therapeutic Applications; Grant number H20c6a0033) and the A\*STAR Central Research Fund (CRF) for generous financial support.

## References

- 1 H. Furukawa, N. Ko, Y. B. Go, N. Aratani, S. B. Choi, E. Choi, A. Ö. Yazaydin, R. Q. Snurr, M. O'Keeffe, J. Kim and O. M. Yaghi, *Science*, 2010, **329**, 424–428.
- 2 S. Kitagawa, R. Kitaura and S.-i. Noro, *Angew. Chem., Int. Ed.*, 2004, **43**, 2334–2375.
- 3 H. Li, M. Eddaoudi, M. O'Keeffe and O. M. Yaghi, *Nature*, 1999, **402**, 276–279.
- 4 O. M. Yaghi, M. O'Keeffe, N. W. Ockwig, H. K. Chae, M. Eddaoudi and J. Kim, *Nature*, 2003, **423**, 705–714.
- 5 S. Kitagawa and R. Matsuda, *Coord. Chem. Rev.*, 2007, **251**, 2490–2509.
- 6 Y. He, W. Zhou, G. Qian and B. Chen, *Chem. Soc. Rev.*, 2014, **43**, 5657–5678.
- 7 J. A. Mason, J. Oktawiec, M. K. Taylor, M. R. Hudson, J. Rodriguez, J. E. Bachman, M. I. Gonzalez, A. Cervellino, A. Guagliardi, C. M. Brown, P. L. Llewellyn, N. Masciocchi and J. R. Long, *Nature*, 2015, **527**, 357–361.
- 8 L. J. Murray, M. Dincă and J. R. Long, *Chem. Soc. Rev.*, 2009, **38**, 1294–1314.
- 9 M. Ding, R. W. Flaig, H.-L. Jiang and O. M. Yaghi, *Chem. Soc. Rev.*, 2019, **48**, 2783–2828.
- 10 J. Lee, O. K. Farha, J. Roberts, K. A. Scheidt, S. T. Nguyen and J. T. Hupp, *Chem. Soc. Rev.*, 2009, **38**, 1450–1459.
- 11 L. E. Kreno, K. Leong, O. K. Farha, M. Allendorf, R. P. Van Duyne and J. T. Hupp, *Chem. Rev.*, 2012, **112**, 1105–1125.
- 12 S. Kitagawa, *Acc. Chem. Res.*, 2017, **50**, 514–516.
- 13 M.-S. Yao, K.-i. Otake, Z.-Q. Xue and S. Kitagawa, *Faraday Discuss.*, 2021, **231**, 397–417.
- 14 G. Maurin, C. Serre, A. Cooper and G. Férey, *Chem. Soc. Rev.*, 2017, **46**, 3104–3107.
- 15 S. Keskin and S. Kizilel, *Ind. Eng. Chem. Res.*, 2011, **50**, 1799–1812.
- 16 P. Horcajada, C. Serre, M. Vallet-Regí, M. Sebban, F. Taulelle and G. Férey, *Angew. Chem., Int. Ed.*, 2006, **45**, 5974–5978.
- 17 P. Horcajada, T. Chalati, C. Serre, B. Gillet, C. Sebrie, T. Baati, J. F. Eubank, D. Heurtaux, P. Clayette, C. Kreuz, J.-S. Chang, Y. K. Hwang, V. Marsaud, P.-N. Bories, L. Cynober, S. Gil, G. Férey, P. Couvreur and R. Gref, *Nat. Mater.*, 2010, **9**, 172–178.
- 18 P. Horcajada, C. Serre, G. Maurin, N. A. Ramsahye, F. Balas, M. Vallet-Regí, M. Sebban, F. Taulelle and G. Férey, *J. Am. Chem. Soc.*, 2008, **130**, 6774–6780.
- 19 W. J. Rieter, K. M. Pott, K. M. L. Taylor and W. Lin, *J. Am. Chem. Soc.*, 2008, **130**, 11584–11585.
- 20 K. M. L. Taylor-Pashow, J. D. Rocca, Z. Xie, S. Tran and W. Lin, *J. Am. Chem. Soc.*, 2009, **131**, 14261–14263.
- 21 W. J. Rieter, K. M. L. Taylor, H. An, W. Lin and W. Lin, *J. Am. Chem. Soc.*, 2006, **128**, 9024–9025.
- 22 H.-S. Wang, *Coord. Chem. Rev.*, 2017, **349**, 139–155.
- 23 M. Bilal, M. Adeel, T. Rasheed and H. M. N. Iqbal, *J. Mater. Res. Technol.*, 2019, **8**, 2359–2371.
- 24 K. Lu, T. Aung, N. Guo, R. Weichselbaum and W. Lin, *Adv. Mater.*, 2018, **30**, 1707634.
- 25 B. V. K. J. Schmidt, *Macromol. Rapid Commun.*, 2020, **41**, 1900333.
- 26 L. Wang, H. Xu, J. Gao, J. Yao and Q. Zhang, *Coord. Chem. Rev.*, 2019, **398**, 213016.
- 27 E. M. Ahmed, *J. Adv. Res.*, 2015, **6**, 105–121.
- 28 Z. P. Liu, S. S. Liow, S. Li Lai, A. Alli-Shaik, G. E. Holder, B. H. Parikh, S. Krishnakumar, Z. B. Li, M. J. Tan, J. Gunaratne, V. A. Barathi, W. Hunziker, R. Lakshminarayanan, C. W. T. Tan, C. K. Chee, P. Zhao, G. Lingam, X. J. Loh and X. Y. Su, *Nat. Biomed. Eng.*, 2019, **3**, 598–610.
- 29 Q. Lin, J. Y. C. Lim, K. Xue, X. Su and X. J. Loh, *Biomaterials*, 2021, **268**, 120547.
- 30 Q. Lin, C. Owh, J. Y. C. Lim, P. L. Chee, M. P. Y. Yew, E. T. Y. Hor and X. J. Loh, *Acc. Mater. Res.*, 2021, **2**, 881–894.
- 31 J. Xiao, S. Chen, J. Yi, H. F. Zhang and G. A. Ameer, *Adv. Funct. Mater.*, 2017, **27**, 1604872.
- 32 H. Z. Liu, H. Peng, Y. M. Xin and J. Y. Zhang, *Polym. Chem.*, 2019, **10**, 2263–2272.
- 33 S. Yuan, L. Feng, K. C. Wang, J. D. Pang, M. Bosch, C. Lollar, Y. J. Sun, J. S. Qin, X. Y. Yang, P. Zhang, Q. Wang, L. F. Zou, Y. M. Zhang, L. L. Zhang, Y. Fang, J. L. Li and H. C. Zhou, *Adv. Mater.*, 2018, **30**, 1704303.
- 34 J. Duan, W. Jin and S. Kitagawa, *Coord. Chem. Rev.*, 2017, **332**, 48–74.



35 N. C. Burtch, H. Jasuja and K. S. Walton, *Chem. Rev.*, 2014, **114**, 10575–10612.

36 A. Zimpel, T. Preiß, R. Röder, H. Engelke, M. Ingrisch, M. Peller, J. O. Rädler, E. Wagner, T. Bein, U. Lächelt and S. Wuttke, *Chem. Mater.*, 2016, **28**, 3318–3326.

37 J. Xiao, Y. Zhu, S. Huddleston, P. Li, B. Xiao, O. K. Farha and G. A. Ameer, *ACS Nano*, 2018, **12**, 1023–1032.

38 N. D. H. Gamage, K. A. McDonald and A. J. Matzger, *Angew. Chem., Int. Ed.*, 2016, **55**, 12099–12103.

39 J. E. Mondloch, O. Karagiaridi, O. K. Farha and J. T. Hupp, *CrystEngComm*, 2013, **15**, 9258–9264.

40 H. D. Lawson, S. P. Walton and C. Chan, *ACS Appl. Mater. Interfaces*, 2021, **13**, 7004–7020.

41 L. Wang, H. Xu, J. Gao, J. Yao and Q. Zhang, *Coord. Chem. Rev.*, 2019, **398**, 213016.

42 T. Kitao, Y. Y. Zhang, S. Kitagawa, B. Wang and T. Uemura, *Chem. Soc. Rev.*, 2017, **46**, 3108–3133.

43 J. Y. C. Lim, S. S. Goh, S. S. Liow, K. Xue and X. J. Loh, *J. Mater. Chem. A*, 2019, **7**, 18759–18791.

44 J. Y. C. Lim, Q. Lin, K. Xue and X. J. Loh, *Mater. Today Adv.*, 2019, **3**, 100021.

45 J. Y. C. Lim, S. S. Goh and X. J. Loh, *ACS Mater. Lett.*, 2020, **2**, 918–950.

46 N. Stock and S. Biswas, *Chem. Rev.*, 2012, **112**, 933–969.

47 M. Safaei, M. M. Foroughi, N. Ebrahimpoor, S. Jahani, A. Omidi and M. Khatami, *TrAC, Trends Anal. Chem.*, 2019, **118**, 401–425.

48 W. Yang, J. Wang, Y. Han, X. Luo, W. Tang, T. Yue and Z. Li, *Food Control*, 2021, **130**, 108409.

49 G. Tan, Y. Zhong, L. Yang, Y. Jiang, J. Liu and F. Ren, *Chem. Eng. J.*, 2020, **390**, 124446.

50 K. Gwon, I. Han, S. Lee, Y. Kim and D. N. Lee, *ACS Appl. Mater. Interfaces*, 2020, **12**, 20234–20242.

51 Z. Li, J. Ren, J. Bu, L. Wang, W. Shi, D. Pan and M. Wu, *J. Electroanal. Chem.*, 2020, **876**, 114489.

52 D.-Y. Gao, Z. Liu and Z.-L. Cheng, *Colloids Surf., A*, 2021, **610**, 125934.

53 M. X. Qiao, D. W. Chen, X. C. Ma and Y. J. Liu, *Int. J. Pharm.*, 2005, **294**, 103–112.

54 G. Z. Tan, Y. T. Zhong, L. L. Yang, Y. D. Jiang, J. Q. Liu and F. Ren, *Chem. Eng. J.*, 2020, **390**, 124446.

55 A. Chakraborty, P. Sutar, P. Yadav, M. Eswaramoorthy and T. K. Maji, *Inorg. Chem.*, 2018, **57**, 14480–14483.

56 S. Javanbakht, A. Hemmati, H. Namazi and A. Heydari, *Int. J. Biol. Macromol.*, 2020, **155**, 876–882.

57 N. Hosono and S. Kitagawa, *Acc. Chem. Res.*, 2018, **51**, 2437–2446.

58 P. Deria, W. Bury, J. T. Hupp and O. K. Farha, *Chem. Commun.*, 2014, **50**, 1965–1968.

59 S. C. Ribeiro, H. H. C. de Lima, V. L. Kupfer, C. T. P. da Silva, F. R. Veregue, E. Radovanovic, M. R. Guilherme and A. W. Rinaldi, *J. Mol. Liq.*, 2019, **294**, 111553.

60 H. H. C. de Lima, C. T. P. da Silva, V. L. Kupfer, J. d. C. Rinaldi, E. S. Kioshima, D. Mandelli, M. R. Guilherme and A. W. Rinaldi, *Carbohydr. Polym.*, 2021, **251**, 116977.

61 W. H. Chen, W. C. Liao, Y. S. Sohn, M. Fadeev, A. Ceconello, R. Nechushtai and I. Willner, *Adv. Funct. Mater.*, 2018, **28**, 1705137.

62 H. Zhu, Q. Zhang and S. P. Zhu, *ACS Appl. Mater. Interfaces*, 2016, **8**, 17395–17401.

63 O. Maan, P. Song, N. X. Chen and Q. Y. Lu, *Adv. Mater. Interfaces*, 2019, **6**, 1801895.

64 S. E. Klein, J. D. Sosa, A. C. Castonguay, W. I. Flores, L. D. Zarzar and Y. Y. Liu, *Inorg. Chem. Front.*, 2020, **7**, 4813–4821.

65 W. Q. Liu, O. Erol and D. H. Gracias, *ACS Appl. Mater. Interfaces*, 2020, **12**, 33267–33275.

66 Y. Zhuang, Y. Kong, X. C. Wang and B. Y. Shi, *New J. Chem.*, 2019, **43**, 7202–7208.

67 Y. Kong, Y. Zhuang, K. Han and B. Y. Shi, *Colloids Surf., A*, 2020, **588**, 124360.

68 L. Qin, R. Ru, J. W. Mao, Q. Meng, Z. Fan, X. Li and G. L. Zhang, *Appl. Catal., B*, 2020, **269**, 118754.

69 Y. J. Du, J. Gao, L. Y. Zhou, L. Ma, Y. He, X. F. Zheng, Z. H. Huang and Y. J. Jiang, *Adv. Sci.*, 2019, **6**, 1970034.

70 T. V. N. Thi, C. L. Luu, T. C. Hoang, T. Nguyen, T. H. Bui, P. H. D. Nguyen and T. P. P. Thi, *Adv. Nat. Sci.: Nanosci. Nanotechnol.*, 2013, **4**, 035016.

71 W. J. Son, J. Kim, J. Kim and W. S. Ahn, *Chem. Commun.*, 2008, 6336–6338, DOI: [10.1039/b814740j](https://doi.org/10.1039/b814740j).

72 Z. Li, J. Ren, J. T. Bu, L. Wang, W. Y. Shi, D. Y. Pan and M. H. Wu, *J. Electroanal. Chem.*, 2020, **876**, 114489.

73 K. Pal, A. K. Banthia and D. K. Majumdar, *Des. Monomers Polym.*, 2009, **12**, 197–220.

74 X. Lian, Y. Zhang, J. M. Wang and B. Yan, *Inorg. Chem.*, 2020, **59**, 10304–10310.

75 Z. Karimzadeh, S. Javanbakht and H. Namazi, *Bioimpacts*, 2019, **9**, 5–13.

76 S. Z. H. Kiadeh, A. Ghaee, M. Farokhi, J. Nourmohammadi, A. Bahi and F. K. Ko, *Int. J. Biol. Macromol.*, 2021, **173**, 351–365.

77 X. Lian and B. Yan, *Chem. Commun.*, 2019, **55**, 241–244.

78 Y. N. Lin, X. Y. Wang, Y. L. Sun, Y. X. Dai, W. Y. Sun, X. D. Zhu, H. Liu, R. Han, D. D. Gao and C. N. Luo, *Sens. Actuators, B*, 2019, **289**, 56–64.

79 C. H. Lin, Y. Du, S. Q. Wang, L. Wang and Y. H. Song, *Mater. Sci. Eng., C*, 2021, **118**, 111511.

80 N. Gao, J. Huang, L. Y. Wang, J. Y. Feng, P. C. Huang and F. Y. Wu, *Appl. Surf. Sci.*, 2018, **459**, 686–692.

81 Y. N. Lin, Y. L. Sun, Y. X. Dai, W. Y. Sun, X. D. Zhu, H. Liu, R. Han, D. D. Gao, C. N. Luo and X. Y. Wang, *Talanta*, 2020, **207**, 120300–120308.

82 J. S. Xiao, S. Y. Chen, J. Yi, H. F. Zhang and G. A. Ameer, *Adv. Funct. Mater.*, 2017, **27**, 1604872.

83 D. L. Han, Y. Li, X. M. Liu, B. Li, Y. Han, Y. F. Zheng, K. W. K. Yeung, C. Y. Li, Z. D. Cui, Y. Q. Liang, Z. Y. Li, S. L. Zhu, X. B. Wang and S. L. Wu, *Chem. Eng. J.*, 2020, **396**, 125194.

84 X. X. Yao, G. S. Zhu, P. G. Zhu, J. Ma, W. W. Chen, Z. Liu and T. T. Kong, *Adv. Funct. Mater.*, 2020, **30**, 1909389.

85 Y. R. Yu, G. P. Chen, J. H. Guo, Y. X. Liu, J. A. Ren, T. T. Kong and Y. J. Zhao, *Mater. Horiz.*, 2018, **5**, 1137–1142.

86 M. Zhang, G. H. Wang, D. Wang, Y. Q. Zheng, Y. X. Li, W. Q. Meng, X. Zhang, F. F. Du and S. X. Lee, *Int. J. Biol. Macromol.*, 2021, **175**, 481–494.

87 S. Yao, J. J. Chi, Y. T. Wang, Y. J. Zhao, Y. Luo and Y. A. Wang, *Adv. Healthcare Mater.*, 2021, **10**, 2100056.

88 J. Huo, J. Aguilera-Sigalat, S. El-Hankari and D. Bradshaw, *Chem. Sci.*, 2015, **6**, 1938–1943.

89 W. Wang, S. Zheng, Y. Hong, X. Xu, X. Feng and H. Song, *ACS Appl. Nano Mater.*, 2022, **5**, 2222–2230.

90 Y. Weng, Z. Song, C.-H. Chen and H. Tan, *Chem. Eng. J.*, 2021, **425**, 131482.

91 Y. Zhang, B.-C. Wang, P. Wang, X.-J. Ju, M.-J. Zhang, R. Xie, Z. Liu, W. Wang and L.-Y. Chu, *React. Chem. Eng.*, 2022, **7**, 275–283.

92 D. Y. Gao, Z. Liu and Z. L. Cheng, *Colloids Surf., A*, 2021, **610**, 125934.

93 C. T. Hsieh, K. Ariga, L. K. Shrestha and S. H. Hsu, *Biomacromolecules*, 2021, **22**, 1053–1064.

94 H. Ji, X. Wang, P. Wang, Y. Gong, Y. Wang, C. Liu, G. Ji, X. Wang and M. Wang, *J. Nanobiotechnol.*, 2022, **20**, 60.

95 J. Li and D. J. Mooney, *Nat. Rev. Mater.*, 2016, **1**, 16071.

96 Z. Ahmad, A. Shah, M. Siddiq and H.-B. Kraatz, *RSC Adv.*, 2014, **4**, 17028–17038.

97 L. Sercombe, T. Veerati, F. Moheimani, S. Y. Wu, A. K. Sood and S. Hua, *Front. Pharmacol.*, 2015, **6**, 286.

98 E. Beltrán-Gracia, A. López-Camacho, I. Higuera-Ciapara, J. B. Velázquez-Fernández and A. A. Vallejo-Cardona, *Cancer Nanotechnol.*, 2019, **10**, 11.

99 A. Laloo, P. Chao, P. Hu, S. Stein and P. J. Sinko, *J. Controlled Release*, 2006, **112**, 333–342.

100 S. S. Liow, Q. Dou, D. Kai, A. A. Karim, K. Zhang, F. Xu and X. J. Loh, *ACS Biomater. Sci. Eng.*, 2016, **2**, 295–316.

101 N. Zhao, L. Yan, X. Zhao, X. Chen, A. Li, D. Zheng, X. Zhou, X. Dai and F.-J. Xu, *Chem. Rev.*, 2019, **119**, 1666–1762.

102 J. Yang and Y.-W. Yang, *Small*, 2020, **16**, 1906846.

103 T. Wen, G. L. Quan, B. Y. Niu, Y. X. Zhou, Y. T. Zhao, C. Lu, X. Pan and C. N. Wu, *Small*, 2021, **17**, 2005064.

104 Z. Dong, Y. Sun, J. Chu, X. Zhang and H. Deng, *J. Am. Chem. Soc.*, 2017, **139**, 14209–14216.

105 M. Nakahama, J. Reboul, K. Yoshida, S. Furukawa and S. Kitagawa, *J. Mater. Chem. B*, 2015, **3**, 4205–4212.

106 S. S. Nagarkar, A. V. Desai and S. K. Ghosh, *Chem. – Asian J.*, 2014, **9**, 2358–2376.

107 W. Cai, J. Wang, C. Chu, W. Chen, C. Wu and G. Liu, *Adv. Sci.*, 2019, **6**, 1801526.

108 L.-L. Tan, H. Li, Y.-C. Qiu, D.-X. Chen, X. Wang, R.-Y. Pan, Y. Wang, S. X.-A. Zhang, B. Wang and Y.-W. Yang, *Chem. Sci.*, 2015, **6**, 1640–1644.

109 X. Meng, B. Gui, D. Yuan, M. Zeller and C. Wang, *Sci. Adv.*, 2016, **2**, e1600480.

110 Y. Kato, S. Ozawa, C. Miyamoto, Y. Maehata, A. Suzuki, T. Maeda and Y. Baba, *Cancer Cell Int.*, 2013, **13**, 89.

111 D. Hanahan and R. A. Weinberg, *Cell*, 2011, **144**, 646–674.

112 W. M. Zapol, H. C. Charles, A. R. Martin, R. C. Sá, B. Yu, F. Ichinose, N. MacIntyre, J. Mammarappallil, R. Moon, J. Z. Chen, E. T. Geier, C. Darquenne, G. K. Prisk and I. Katz, *J. Aerosol Med. Pulm. Drug Delivery*, 2018, **31**, 78–87.

113 J. S. Beckman and W. H. Koppenol, *Am. J. Physiol.: Cell Physiol.*, 1996, **271**, C1424–C1437.

114 A. K. Mustafa, M. M. Gadalla, N. Sen, S. Kim, W. Mu, S. K. Gazi, R. K. Barrow, G. Yang, R. Wang and S. H. Snyder, *Sci. Signaling*, 2009, **2**, ra72.

115 A. C. McKinlay, B. Xiao, D. S. Wragg, P. S. Wheatley, I. L. Megson and R. E. Morris, *J. Am. Chem. Soc.*, 2008, **130**, 10440–10444.

116 P. Bhatraju, J. Crawford, M. Hall and J. D. Lang, *Nitric Oxide*, 2015, **50**, 114–128.

117 F. Murad, *Angew. Chem., Int. Ed.*, 1999, **38**, 1856–1868.

118 D. Ma, S. Wilhelm, M. Maze and N. P. Franks, *Br. J. Anaesth.*, 2002, **89**, 739–746.

119 S. M. Fix, M. A. Borden and P. A. Dayton, *J. Controlled Release*, 2015, **209**, 139–149.

120 S.-L. Huang, D. D. McPherson and R. C. MacDonald, *Ultrasound Med. Biol.*, 2008, **34**, 1272–1280.

121 S. Diring, D. O. Wang, C. Kim, M. Kondo, Y. Chen, S. Kitagawa, K.-i. Kamei and S. Furukawa, *Nat. Commun.*, 2013, **4**, 2684.

122 C. Kim, S. Diring, S. Furukawa and S. Kitagawa, *Dalton Trans.*, 2015, **44**, 15324–15333.

123 S. Diring, A. Carné-Sánchez, J. Zhang, S. Ikemura, C. Kim, H. Inaba, S. Kitagawa and S. Furukawa, *Chem. Sci.*, 2017, **8**, 2381–2386.

124 F. P. Kinik, A. Ortega-Guerrero, D. Ongari, C. P. Ireland and B. Smit, *Chem. Soc. Rev.*, 2021, **50**, 3143–3177.

125 P. I. Scheurle, A. Mähringer, A. C. Jakowetz, P. Hosseini, A. F. Richter, G. Wittstock, D. D. Medina and T. Bein, *Nanoscale*, 2019, **11**, 20949–20955.

126 Y. Takashima, V. M. Martínez, S. Furukawa, M. Kondo, S. Shimomura, H. Uehara, M. Nakahama, K. Sugimoto and S. Kitagawa, *Nat. Commun.*, 2011, **2**, 168.

127 M. D. Allendorf, C. A. Bauer, R. K. Bhakta and R. J. T. Houk, *Chem. Soc. Rev.*, 2009, **38**, 1330–1352.

128 L. Li, J. Y. Zou, S. Y. You, Y. W. Liu, H. M. Cui and S. W. Zhang, *Dyes Pigm.*, 2020, **173**, 108004.

129 K. S. Asha, R. Bhattacharjee and S. Mandal, *Angew. Chem., Int. Ed.*, 2016, **55**, 11528–11532.

130 H. Q. Xie and Y. J. Kang, *Curr. Med. Chem.*, 2009, **16**, 1304–1314.

131 V. Coger, N. Million, C. Rehbock, B. Sures, M. Nachev, S. Barcikowski, N. Wistuba, S. Strauss and P. M. Vogt, *Biol. Trace Elem. Res.*, 2019, **191**, 167–176.

132 E. Larraneta, R. E. M. Lutton, A. D. Woolfson and R. F. Donnelly, *Mater. Sci. Eng., R*, 2016, **104**, 1–32.

133 X. Lian, Y. Fang, E. Joseph, Q. Wang, J. Li, S. Banerjee, C. Lollar, X. Wang and H.-C. Zhou, *Chem. Soc. Rev.*, 2017, **46**, 3386–3401.

134 Y. Liu, T. Jiang and Z. Liu, *Nanotheranostics*, 2022, **6**, 2206–7418.

135 S. K. Thakur, D. P. Singh and J. Choudhary, *Cancer Metastasis Rev.*, 2020, **39**, 989–998.

136 C. H. Park, K. Han, J. Hur, S. M. Lee, J. W. Lee, S. H. Hwang, J. S. Seo, K. H. Lee, W. Kwon, T. H. Kim and B. W. Choi, *Chest*, 2017, **151**, 316–328.

137 W. Liu, O. Erol and D. H. Gracias, *ACS Appl. Mater. Interfaces*, 2020, **12**, 33267–33275.

138 Y. Zhuang, Y. Kong, X. Wang and B. Shi, *New J. Chem.*, 2019, **43**, 7202–7208.

139 O. Maan, P. Song, N. Chen and Q. Lu, *Adv. Mater. Interfaces*, 2019, **6**, 1801895.

140 C. Fu, H. Zhou, L. Tan, Z. Huang, Q. Wu, X. Ren, J. Ren and X. Meng, *ACS Nano*, 2018, **12**, 2201–2210.

141 J. Oyim, C. A. Omolo and E. K. Amuhaya, *Front. Chem.*, 2021, **9**, 635344–635344.

142 X. Zhang, L. Fang, K. Jiang, H. He, Y. Yang, Y. Cui, B. Li and G. Qian, *Biosens. Bioelectron.*, 2019, **130**, 65–72.

143 N. Bhardwaj, S. K. Bhardwaj, J. Mehta, K.-H. Kim and A. Deep, *ACS Appl. Mater. Interfaces*, 2017, **9**, 33589–33598.

144 N. Bhardwaj, S. K. Bhardwaj, D. Bhatt, S. K. Tuteja, K.-H. Kim and A. Deep, *Anal. Methods*, 2019, **11**, 917–923.

145 N. Singh, S. Qutub and N. M. Khashab, *J. Mater. Chem. B*, 2021, **9**, 5925–5934.

146 T. Simon-Yarza, A. Mielcarek, P. Couvreur and C. Serre, *Adv. Mater.*, 2018, **30**, 1707365.

147 S. L. Anderson and K. C. Stylianou, *Coord. Chem. Rev.*, 2017, **349**, 102–128.

148 J. An, S. J. Geib and N. L. Rosi, *J. Am. Chem. Soc.*, 2009, **131**, 8376–8377.

149 J. An, C. M. Shade, D. A. Chengelis-Czegan, S. Petoud and N. L. Rosi, *J. Am. Chem. Soc.*, 2011, **133**, 1220–1223.

150 M. Rubio-Martinez, C. Avci-Camur, A. W. Thornton, I. Imaz, D. MasPOCH and M. R. Hill, *Chem. Soc. Rev.*, 2017, **46**, 3453–3480.

151 A. Mandal, J. R. Clegg, A. C. Anselmo and S. Mitragotri, *Bioeng. Transl. Med.*, 2020, **5**, e10158.